6.2 REAL-DATA AND IDEALIZED SIMULATIONS OF THE 4 JULY 2004 BOW ECHO EVENT

Kent H. Knopfmeier*, Robert J. Trapp, and Dustan M. Wheatley
Purdue University, West Lafayette, IN

1. INTRODUCTION

The propensity of bowing convective line segments to produce severe weather was first recognized in the early studies of Nolen (1959) and Hamilton (1970). Fujita (1978) coined these segments “bow echoes” and provided the first conceptual model that described their evolution from strong, tall echo to bow echo due to intense downdrafts near the bow echo apex. Later studies (e.g., Smull and Houze 1987; Jorgensen and Smull 1993) linked these downdrafts, and thus damaging surface winds, to a descending rear-inflow jet (RIJ).

Recent idealized simulations (e.g. Trapp and Weisman 2003) have shown the most intense damaging winds, compared to those produced by the RIJ within a given convective system, are induced by low-level mesovortices. Observational evidence (e.g. Atkins et al. 2005; Wheatley et al. 2005) has confirmed the proposed mesovortex-high wind association.

Although the mechanisms for damaging wind production within bow echoes have been clarified through several observational and numerical studies, limited research exists (e.g. Bernardet and Cotton 1998) on the processes that bring these winds to the surface when a stable, nocturnal planetary boundary layer (PBL) is present.

The influence of external surface boundaries (e.g. remnant outflow) on bow echo evolution is another incomplete area in severe local storm research. Observational studies (e.g. Klimowski et al. 2000; Przybylinski et al. 2000; Schmocker et al. 2000) have documented how bow-echo boundary interaction can influence bow echo and mesovortex formation and subsequent morphology. However, this work fails to elucidate the dynamics and the specific effects of the interaction.

The ultimate goal of the present study is to address both issues through analysis and simulation of the 4 July 2004 bow echo that occurred in the central United States. This bow echo produced a long swath of straight-line wind damage and an F1 tornado along its path from southeastern Kansas through northern Alabama. Lese (2006) provides a radar analysis from the perspective of the Springfield, MO (KSGF) WSR-88D, and additionally describes some of the warning operations issues raised by event. Our focus in this article is the formation of an externally produced outflow boundary and its eventual interaction with the bow echo. Observational data and real-data WRF simulation results depicting this progression are compared and contrasted. Also, through the idealized WRF configuration, the effects of a homogeneous environment on bow echo formation and evolution are presented.

2. ENVIRONMENTAL OVERVIEW

The synoptic and mesoscale conditions during the early morning hours of 4 July 2004 were fairly typical of early summer in the Central Plains. Minimal synoptic scale forcing was present in the genesis region, along with weak low-level (~ 5 m s^{-1} at 850 hPa) and mid-level (~ 13 m s^{-1} at 500 hPa) winds. The 1200 UTC KSGF sounding (not shown) exhibited this weak shear (~ 14 m s^{-1} over the lowest 6 km), but also revealed relatively high surface-based convective available potential energy (SBCAPE) values (~ 1040 J/kg) for the time of day (0700 LDT). Also evident from the sounding was the strong nocturnal inversion present in the area, which

* *Corresponding author address*: Kent H. Knopfmeier, Purdue Univ., Department of Earth and Atmospheric Sciences, West Lafayette, IN, 47907-2051; email: kknopfme@purdue.edu

resulted in large convective inhibition (CIN) values (~ 300 J/kg).

3. OBSERVED BOUNDARY AND BOW ECHO EVOLUTION

The observed boundary was the result of rain-cooled outflow from convection that formed along the Colorado-Wyoming border at approximately 1900 UTC 3 July 2004. As the convection moved eastward into extreme northeastern Colorado/ southwestern Nebraska at 2200 UTC, a reflectivity fine line became visible on the Goodland, KS WSR-88D, indicating the presence of the rather extensive boundary. By 0000 UTC 4 July 2004, this feature had dropped farther south and was located from central Nebraska through eastern Colorado. Convection continually developed along the boundary through 0500 UTC as it moved farther eastward into extreme southeastern Nebraska and central Kansas (Fig. 1). By 0730 UTC, the northern half of the boundary accelerated farther east, while the southern half had dropped slowly south into east- and south-central Kansas. Strong convective cells formed along a line just to the north of the boundary and through cell mergers and presumably cold pool dynamics, an intense, albeit compact bow echo developed. The original boundary was still visible from the KSGF WSR-88D when the bow echo reached maximum intensity near 1200 UTC (Fig. 2). This was also the period during which a mesovortex was evident near the intersection of the boundary and bow echo. Interaction between the two features began near 1100 UTC and continued through 1400 UTC, as the system weakened.

Fig. 1 summarizes the inextricable link between the outflow boundary and bow echo. Indeed, the long-lived boundary not only aided in the development of the convective system, but also appeared to play a role in its eventual severity.

4. REAL-DATA MODELING METHODOLOGY

Owing to the unavailability of any special field observations of the 3D structure of the bow echo or boundary, we turn to the WRF Version 2.1.2 modeling system to aid in the investigation of this event. An interactive, two-way nested framework (Fig. 3) was employed in order to capture the boundary and bow echo evolution within high resolution domains. The outermost domain (d01) has a horizontal gridpoint spacing of 9 km with Kain-Fritsch (KF) cumulus parameterization activated. The first nested domain (d02) has a horizontal gridpoint spacing of 3 km and was placed to ensure deep, moist convection would occur solely on this domain. The innermost domain (d03) with a horizontal resolution of 1 km was enacted to provide high definition in the area where both bow echo-boundary interaction and mesovortex formation occurred. Table 1 summarizes the model configuration utilized in this study.

The model was initialized at 0000 UTC 4 July 2004 using the 40 km Eta model forecast as boundary conditions, which were updated on a 3 h interval. The model was integrated in time to 0000 UTC 5 July.

Table 1. Summary of WRF model configuration utilized in this study.

WRF V2.1.2 Model Configuration	
Domains (Grid Spacing)	d01 (9 km) d02 (3 km) d03 (1 km)
Vertical Levels	31
Microphysics	Purdue Lin
Cumulus	Kain-Fritsch (d01 only)
Longwave Radiation	RRTM
Shortwave Radiation	Dudhia
Surface Layer Physics	Monin-Obukhov (Janjic Eta)
Surface Layer	Noah LSM
Boundary Layer Physics	Mellor-Yamada-Janjic (MYJ)

5. REAL-DATA SIMULATION RESULTS

The WRF simulation successfully reproduced the many features associated with the observed event, including the formation and evolution of a boundary, the initiation of a bow echo, the bow echo-boundary interaction, and the development of mesovortices. A more detailed description of the model results in terms of the above features follows.

5.1. Bow Echo and Boundary Evolution

Two boundaries, both associated with cool thunderstorm outflow, were evident in the numerical simulation by 0300 UTC, 3 h after model initialization. One (B1) has propagated south out of south-central Nebraska, while another (B2) has moved east out of the Oklahoma-Texas panhandle. At 0600 UTC (Fig. 4a), B1 was located in an arc through central and northeastern Kansas, while B2 stretched from south-central Kansas into northern Oklahoma, with convection initiating along both boundaries. By 0800 UTC (Fig. 4b), B1 and B2 began to interact in south-central Kansas. Convection continued to be evident along both boundaries. During the period from 0800-1000 UTC, B1 began to stall along a line from west-central Missouri through southern KS, while B2 continued to move eastward. A narrow line of convection formed and consolidated during this time period, reaching southeastern KS by 1000 UTC (Fig. 4c). From 1000-1100 UTC, the system reached its maximum intensity and the convective line exhibited a gradual bowing with a fairly pronounced apex at 1100 UTC (Fig. 4d). After 1100 UTC, B1 quickly lost its identity and the interaction with the now rapidly weakening bow echo ceased.

5.2. Mesovortexgenesis

Mesovortices were evident at 0945, 1000, and 1115 UTC. At 1115 UTC, B1 exhibited clear interaction with the bow echo in the vicinity of a mesovortex (i.e. Fig. 5). The mesovortex contained vorticity values greater than 0.01 s^{-1} (maximum of 0.013 s^{-1}) over a depth of 2 km with a diameter of 5 km.

5.3. Comparison between Observed and Modeled System

It is appropriate to note here that most simulated features compared remarkably well with the observations. The evolution of B1 (Fig. 6), the development of the mesovortex near the bow-echo boundary interaction, and the interaction itself were nearly spatially and temporally correct. However, B2, along with its associated convection, were absent from the observations. The observed bow echo initiated fully from convection behind the boundary originating in south-central Nebraska. The development of the simulated bow echo appeared to be influenced heavily by convection associated with B2. Subsequently, however, the simulated bow echo evolved much like the observed bow echo.

6. IDEALIZED SIMULATIONS

6.1. Purpose

The real-data simulations and observations both suggest a dependence of key bow echo characteristics, such as a low-level mesovortex, on the long-lived boundary. Idealized simulations are now utilized to assess whether a homogenous atmosphere, that is, one without this external boundary, could still support the formation of the bow echo characteristics. Through the use of a sounding representative of the pre-convective environment from the real-data simulations, the idealized simulations attempt to produce an intense, long-lived bow echo in an initially horizontally uniform environment.

6.2. Modeling Methodology

The WRF Version 2.1.2 modeling system in an idealized framework is employed with a base atmospheric state dictated by the representative sounding, as noted above. Convection was initiated by a line of five thermal perturbations, each with a temperature excess of 5 K, a radius of 20 km, and spaced a distance of 40 km. Each simulation is integrated for 6 h.

Table 2 depicts the variables altered during the suite of idealized simulations. Beginning from the control experiment, whereby the representative sounding is unaltered, each variable is then introduced while holding all others constant.

6.3. Results

The idealized simulations reveal an inability of this homogenous environment to produce an intense, long-lived bow echo and induce mesovortexgenesis. No configuration initiated a system comparable to either the observed or real-data modeled bow echo. Fig. 7 is an example of one of the many similar systems that evolved during the series of experiments. The strongest convection is confined to the center of the system 3 h into the simulation. Subsequently, morphology into an intense bow echo fails to occur, and no mesovortices develop.

7. CONCLUSIONS AND FUTURE WORK

The results presented herein prove the ability of the WRF model to simulate features associated with quasi-linear convective systems, such as bow echoes. Specifically, it produced a bow echo, captured its interaction with an externally produced outflow boundary, and resolved a significant mesovortex with excellent spatial and temporal accuracy when compared with the observed. Also, the idealized simulations reveal the insufficiency of the representative atmosphere to initiate a severe, long-lived bow echo.

Future work will involve continued exploration of the bow-echo boundary interaction, as it may represent the key mechanism that first initiates bow echo formation, and then induces mesovortex development. Investigating the mechanism(s) responsible for sustaining the long-lived boundary will be examined. Further quantification of necessity versus sufficiency in terms of an inhomogeneous environment for bow echo formation will also be completed.

8. REFERENCES

Atkins, N. T., C. Bouchard, R.J. Trapp, R. W. Pryzbylinski, and G. K. Schmocker, 2005: Damaging surface wind mechanisms within the 10 June 2003 St. Louis bow echo event during BAMEX. *Mon. Wea. Rev.*, **133**, 2275-2296.

Bernardet, L. R., and W. R. Cotton., 1998: Multiscale Evolution of a Derecho-Producing Mesoscale Convective System. *Mon. Wea. Rev.*, **126**, 2991–3015.

Fujita, T. T., 1978: Manual of downburst identification for project Nimrod. Satellite and Mesometeorology Research Paper 156, Dept. of Geophysical Science, University of Chicago, 104 pp.

Hamilton, R.E., 1970: Use of detailed intensity radar data in mesoscale surface analysis of the 4 July 1969 storm in Ohio. Preprints, *14th Conf. on Radar Meteorology,* Tucson, AZ, Amer. Meteor. Soc., 339-342

Jorgensen, D. P., and B. F. Smull, 1993: Mesovortex circulations seen by airborne Doppler radar within a bow-echo mesoscale convective system. *Bull. Amer. Meteor. Soc.,* **74**, 2146-2157.

Lese, A., 2006: Observations and quantification of low-level mesovortex evolution within the 4 July 2004 southwest Missouri high wind event. Preprints, *23rd Conf. on Severe Local Storms*, St. Louis, MO, Amer. Meteor. Soc., [this volume].

Nolen, R.H., 1959: A radar pattern associated with tornadoes. *Bull. Amer. Meteor. Soc.*, **40,** 277-279.

Smull, B. F., and R. A. Houze, Jr., 1987: Rear inflow in squall lines with trailing stratiform precipitation. *Mon. Wea. Rev.,* **115**, 2869-2889.

Trapp, R. J., and M. L. Weisman, 2003: Low level mesovortices within squall lines and bow echoes. Part II: Their genesis and implications. *Mon. Wea. Rev.*, **131**, 2804-2823.

Wheatley, D. M., R. J. Trapp, and N. T. Atkins, 2006: Radar and damage analysis of severe bow echoes observed during BAMEX. *Mon. Wea. Rev.*, **134,** 791-806.

9. FIGURES AND TABLES

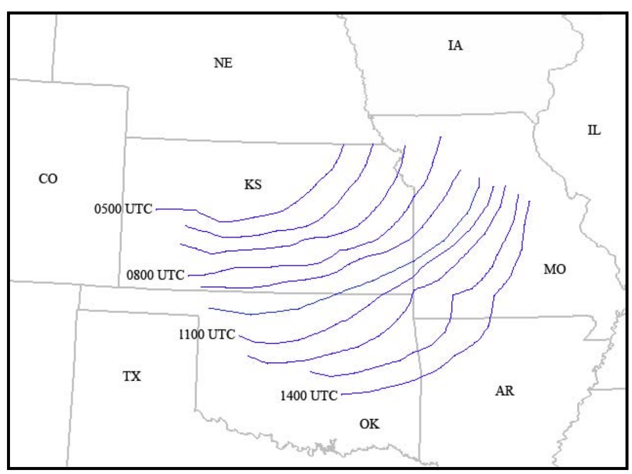

Fig. 1. Isochrones of observed boundary evolution from 0500 UTC to 1400 UTC 4 July 2004.

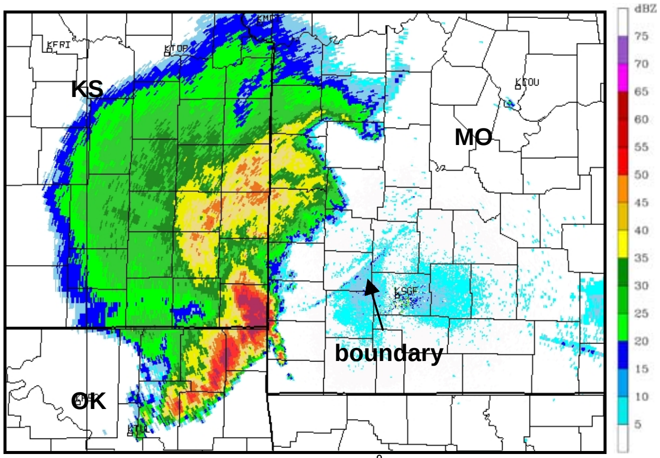

Fig. 2. Level II base reflectivity (0.5° elevation) image from the KSGF WSR-88D at 1201 UTC 4 July 2004.

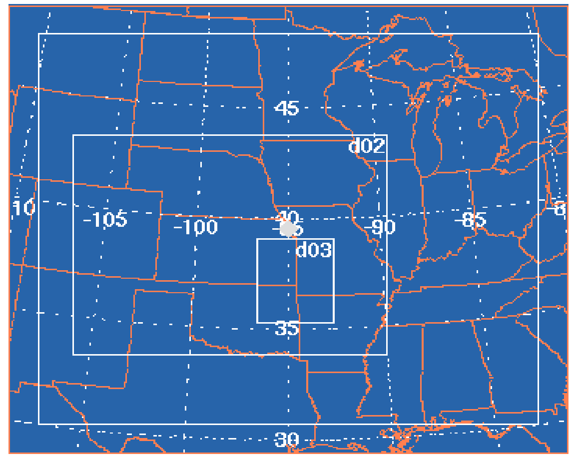

Fig. 3. WRF integration domain used to simulate the bow echo of 4 July 2004.

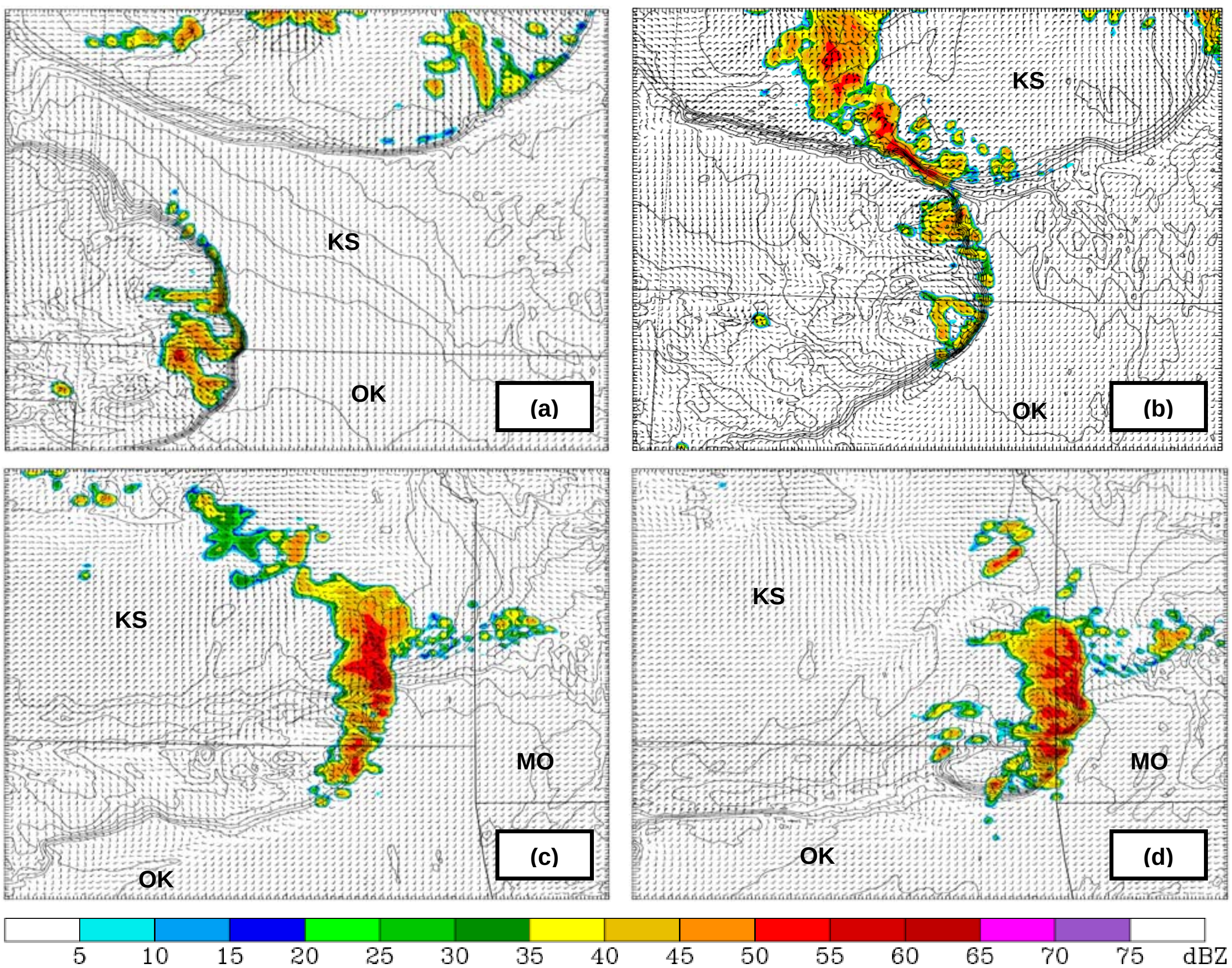

Fig. 4. Horizontal cross sections of simulated reflectivity (dBz; see label bar), equivalent potential temperature (Θ_e) (solid black lines; contour interval of 3 K), and winds (full barb has a speed of 5 m s^{-1}) at the lowest model vertical level at (a) 0600 UTC, (b) 0800 UTC, (c) 1000 UTC, and (d) 1100 UTC 4 July 2004.

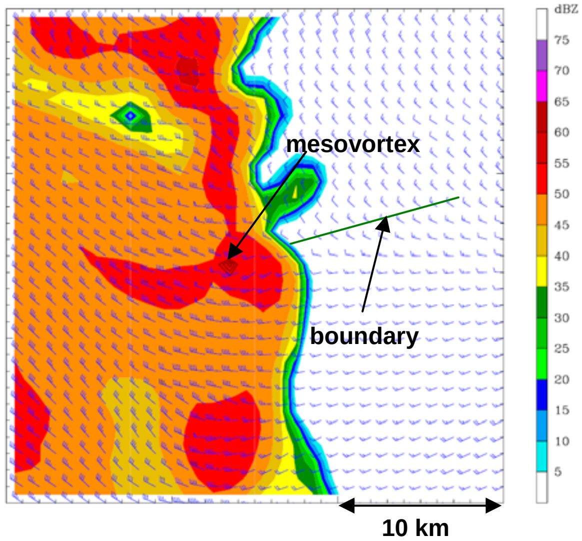

Fig. 5. Horizontal cross sections of simulated reflectivity (dBz; see label bar), vertical vorticity (solid black lines; contour interval of 0.001 s^{-1}), and winds (full barb has a speed of 5 m s^{-1}) at the lowest model vertical level at 1115 UTC 4 July 2004.

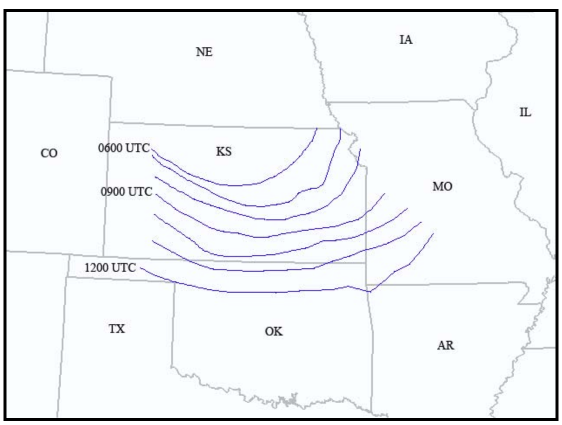

Fig. 6. Isochrones of modeled boundary location from 0600 UTC to 1200 UTC 4 July 2004.

Table 2. Summary of Idealized WRF Experiments

300 X 300 km Domain	
Modifications	**Variability**
None (Control)	
Bubble Line Orientation	**45°** **Along x-axis**
Bubble Diameter	**20 km** **40 km**
Bubble Location	**Western Edge** **Southwestern Edge**
Coriolis Forcing	**None** **10^{-4}**
Wind Profile	**Unidirectional (270°) w/ 20 m/s shear over lowest 2.75 km** **Unidirectional (270°)** **Rotated to produce a shear vector perpendicular to initial bubbles**
Thermodynamic Profile	**CIN removed**
600 X 600 km Domain	
Modifications	**Variability**
None (Control)	
Thermal Perturbation	**2.5 K** **5 K** **10 K**
Bubble Diameter	**40 km**
Wind Profile	**Rotated to produce a shear vector perpendicular to initial bubbles**
Coriolis Forcing	**None** **10^{-4}**

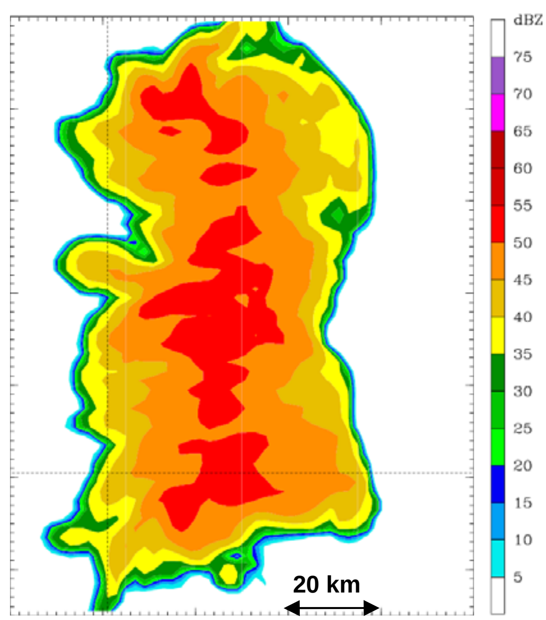

Fig. 7. Horizontal cross section of simulated reflectivity (dBz; see label bar) 3 h into the simulation at the lowest model vertical level.